

A simulational and theoretical study of the spherical electrical double layer for a size-asymmetric electrolyte: the case of big coions.

G. Iván Guerrero-García,¹ Enrique González-Tovar,¹ and Martín Chávez-Páez¹

¹*Instituto de Física, Universidad Autónoma de San Luis Potosí,
Álvaro Obregón 64, 78000 San Luis Potosí, San Luis Potosí, México*

(Dated: March 25, 2021)

Monte Carlo simulations of a spherical macroion, surrounded by a size-asymmetric electrolyte in the primitive model, were performed. We considered 1:1 and 2:2 salts with a size ratio of 2 (i.e., with coions twice the size of counterions), for several surface charge densities of the macro-sphere. The radial distribution functions, electrostatic potential at the Helmholtz surfaces, and integrated charge are reported. We compare these simulational data with original results obtained from the Ornstein-Zernike integral equation, supplemented by the hypernetted chain/hypernetted chain (HNC/HNC) and hypernetted chain/mean spherical approximation (HNC/MSA) closures, and with the corresponding calculations using the modified Gouy-Chapman and unequal-radius modified Gouy-Chapman theories. The HNC/HNC and HNC/MSA integral equations formalisms show good concordance with Monte Carlo “experiments”, whereas the notable limitations of point-ion approaches are evidenced. Most importantly, the simulations confirm our previous theoretical predictions of the non-dominance of the counterions in the size-asymmetric spherical electrical double layer [J. Chem. Phys. **123**, 034703 (2005)], the appearance of anomalous curvatures at the outer Helmholtz plane and the enhancement of charge reversal and screening at high colloidal surface charge densities due to the ionic size asymmetry.

PACS numbers: 61.20.Gy, 61.20.Ja, 61.20.Ne, 61.20.Qg.

I. INTRODUCTION

The study of charged colloidal solutions is very relevant for both basic research and technology due to the ubiquitous nature of these systems [1, 2, 3, 4, 5, 6]. Accordingly, the attainment of a successful theoretical description of such state of matter should represent a keystone for later developments in colloid science. For many years, the scientific community has investigated the structural characteristics of these materials, trying to understand the role of the electrostatic and entropic correlations in their observable properties. In particular, the interest in charged suspensions has prompted the burgeoning of unprecedented experimental techniques and of numeric and statistical mechanics approaches of increasing complexity. On the theoretical side, and despite of the notorious progress in the speed of machine calculations, at present, it is not yet possible to mimic a real dispersion without making several and important simplifications in order to establish a tractable problem. Thus, for example, one of the most elemental idealizations of a diluted charged colloidal suspension is the combination of the cell and primitive models. Within this scheme, the average distance between non-concentrated macroions bathed by an electrolyte is very large, and therefore it is expected that the thermodynamics of the system will depend mainly on the ionic structure, or electrical double layer (EDL), around a single macroparticle enclosed in an electroneutral cell. Complementarily, the so-called primitive model (PM), in which the ions are treated as hard spheres with punctual charges embedded in their centers and the solvent is considered a continuous medium, stands as the most thriving representation of a multi-component elec-

trollyte. A particular case of the PM is the restricted primitive model (RPM), where all the ionic species are of equal size. This condition drastically facilitates the theoretical analysis and, as a consequence, a great amount of work has been performed in the RPM for the planar [7, 8, 9, 10, 11, 12], cylindrical [13, 14, 15, 16] and spherical [17, 18, 19, 20, 21, 22, 23] double layers. In strong contrast, there are few articles in which the effects of ionic size asymmetry have been studied systematically, and these publications focus chiefly on the planar instance [24, 25, 26, 27, 28, 29, 30, 31, 32, 33, 34, 35, 36].

Certainly, the widespread use of the RPM to examine the double layer has led to significant advances in the field, mainly due to its ability to explain a large variety of colloidal phenomena, and, therefore, has established it as the standard representation of the EDL. In turn, this adequacy suggests that the RPM already contains most of the fundamental traits of a colloidal suspension at the usual conditions of experiments and applications. However, we consider that the lack of interest in upgrading the model of a double layer so as to incorporate the effect of ionic size asymmetry stems not only from the operational advantages and/or from the past success of the RPM but also has been influenced by the common belief in the *dominance of the counterions* in the EDL. Such credence has its probable origin in a pioneering Poisson-Boltzmann (PB) study by Valleau and Torrie [24], where they stated the following: “...we expect the double layer properties of a dilute (size-asymmetric) electrolyte to become similar to those of a completely symmetric electrolyte having an effective size equal to that of the counterion. (This remark will be asymptotically exact for large fields in the Poisson-Boltzmann theory)...”.

To be more explicit, in Ref. [24] a size-asymmetric electrolyte next to an electrified wall was analyzed via a *quasi point-like ions* theory known as unequal-radius modified Gouy-Chapman (URMGC), which in essence is equivalent to the classical nonlinear PB equation for a binary mixture of punctual ions but with the assignment of different distances of closest approach (with respect to the plate) to anions and cations. Therefore, the remark of counterion dominance, quoted above, was indeed formulated and proved strictly at the Poisson-Boltzmann level.

Notably, during the past years, a great deal of modern treatments of the EDL have also endorsed the idea that counterions control the properties of high charged surfaces immersed in both size-symmetric [22, 37, 38] and size-asymmetric [27, 28, 31, 32] primitive model (RPM and PM, respectively) electrolytes. Such agreement, about the dominance of counterions, between the current EDL theories and the old URMGC picture is remarkable since in all these new integral equations [27, 28, 31, 37], density functional [22, 32] and mean electrostatic potential [38] papers the fundamental hypothesis of point-ions has been surpassed by including explicitly the hard-core and electrostatic correlations neglected in the PB theory. Notwithstanding, it must be noted that in the cited beyond-PB surveys the “confirmation” of the leading role of counterions has been based in studies of either charge-asymmetric RPM electrical double layers at low/moderate surface charges [37] or, else, of size-asymmetric systems near the point of zero charge (PZC) [27, 31, 37]. In other words, therein the original conclusion of the preponderance of counterions in the EDL at *high* electric fields has not been really tested.

In this context, very recently, some of the present authors have reported the first theoretical investigation of the size-asymmetric spherical electrical double layer (SEDL) [33], where it was found that, contrary to the accepted common opinion, for large macrosphere’s charge densities *the counterions do not dominate*. As a matter of fact, coions are so important that their size can induce drastic correlations that bring forth considerable changes in the EDL’s potential-charge relationship and the surge of the charge reversal phenomenon in monovalent salts. Remarkably, in the same Ref. [33], the correctness of the novel hypernetted chain/mean spherical approximation (HNC/MSA) account of the size-asymmetric SEDL was already verified, *at the level of the radial distribution functions* (RDFs), after comparing favorably a few Monte Carlo and molecular-dynamics simulations of the ionic density profiles with the corresponding HNC/MSA integral equation results. Nevertheless, even if this positive checking of the HNC/MSA RDFs foresees that other ensuing theoretical predictions (e.g. the non-dominance of the counterions and the anomalous behavior of the electrostatic potential at the outer Helmholtz plane) could be true, it would be beneficial to have a specific and more exhaustive delving of these new features by means of refined computer “experiments” and/or alternative theories (i.e. integral equations, density functionals or mean

electrostatic potential schemes). Precisely, the primary objective of this communication is to extend the research of the size-asymmetric SEDL of Ref. [33] by providing fresh and comprehensive simulational and theoretical information that corroborates the enhancement of the neutralization and the screening previously found by the theory and, principally, the non-dominance of counterions at high colloidal charges.

The structure of this paper is as follows: the molecular model of the SEDL, theories and Monte Carlo simulations are described in Sec. II. In Sec. III the partial effects of the electrolytic size asymmetry in the nonlinear Poisson-Boltzmann scheme via, the URMGC approach are discussed, in order to establish a stand point to compare and discuss the role of the ionic size and size asymmetry when these features are included *consistently* in the MC simulations and in the integral equations theory, in the HNC/MSA and HNC/HNC approximations. To end, a summary of the main findings and some concluding remarks are given in Sec. IV.

II. MODEL AND THEORY

A. Molecular model

The main results of this paper are based on the following representation of the spherical electrical double layer (SEDL), which is constituted by a rigid, charged spherical colloid of diameter D and surface charge density σ_0 , surrounded by a continuum solvent of dielectric constant ϵ . The macroion is in contact with two ionic species, which are treated as hard spheres of *diameters* R_i ($i = 1, 2$) with embedded point charges of valences z_i at their centers. Without loss of generality, we consider that $R_2 \geq R_1$. The interaction potential between the macroion, M , and an ion of type i is then given by

$$U_{Mi}(r) = \begin{cases} \infty, & r < \frac{D+R_i}{2}, \\ \frac{z_i e (\frac{D}{2})^2 \sigma_0}{\epsilon_0 \epsilon r}, & r \geq \frac{D+R_i}{2}, \end{cases} \quad (1)$$

where e is the protonic charge. In turn, the interaction potential between two ions of species i and j is given by

$$U_{ij}(r) = \begin{cases} \infty, & r < \frac{R_i+R_j}{2}, \\ \frac{z_i z_j e^2}{4\pi \epsilon_0 \epsilon r}, & r \geq \frac{R_i+R_j}{2}. \end{cases} \quad (2)$$

In the classic literature, the Stern layer or, more properly, the Helmholtz *surface* is the geometrical place corresponding to the closest approach distance between the electrolyte ions and the colloid. If we consider an electrolyte formed by a pair of ionic species of *unequal* size, the inner Helmholtz plane (IHP) is determined by $(D + R_1)/2$, i.e. by the closest approach distance of the smallest component to the surface, whereas the outer

Helmholtz plane (OHP) is established by $(D + R_2)/2$, which corresponds to the distance of closest approach for the largest species. In the limit of identical sizes the IHP and OHP coincide and the usual definition of the Helmholtz plane is recovered.

B. The HNC/HNC and HNC/MSA integral equations for the PM-SEDL

The structural properties of the electrical double layer can be obtained from the Ornstein-Zernike equation for a multicomponent mixture of S species, which is:

$$h_{ij}(r_{12}) = c_{ij}(r_{12}) + \sum_{l=1}^S \rho_l \int h_{il}(r_{13}) c_{lj}(r_{32}) dV. \quad (3)$$

The set of equations (3) requires a second relation, or closure, for the functions $h_{ij}(r)$ and $c_{ij}(r)$. For charged systems, the HNC and MSA closures are widely used. These relations are given by

$$c_{ij}(r_{12}) = -\beta U_{ij}(r_{12}) + h_{ij}(r_{12}) - \ln(h_{ij}(r_{12}) + 1), \quad (4)$$

for HNC, and

$$c_{ij}(r_{12}) = -\beta U_{ij}(r_{12}), \quad (5)$$

for MSA, with

$$i, j = 1, 2 \dots S.$$

These expressions are complemented by the exact condition $h_{ij} = -1$ when $r_{ij} < R_{ij}$, such as $R_{ij} = (R_i + R_j)/2$.

Let us consider that the species S corresponds to macroions at infinite dilution in a binary electrolyte. Then Eqs. (3) for species $S \equiv M$ and j can be written as:

$$h_{Mj}(r_{12}) = c_{Mj}(r_{12}) + \sum_{l=1}^2 \rho_l \int h_{Ml}(r_{13}) c_{lj}(r_{32}) dV. \quad (6)$$

$j = 1, 2.$

When Eq. (4) is used in (6) for both $c_{Mj}(r)$ and $c_{ij}(r)$ the HNC/HNC integral equation is obtained for the SEDL. Besides, if Eq. (4) is employed in Eq. (6) only for $c_{Mj}(r)$, and the $c_{ij}(r)$ are approximated by the corresponding MSA bulk expressions (i.e. Eq. (5) is inserted in Eq. (3) for the two electrolytic species), the HNC/MSA integral equation is established. The details of these integral equations formalisms can be consulted elsewhere [17, 33, 39] and will not be repeated here. However, it is important to mention that both schemes satisfy the global electroneutrality condition.

As an especial case of HNC/MSA, if $R_1 = R_2 = 0$ in Eq. (2), and $R_1 \neq 0$ and $R_2 \neq 0$ in Eq. (1), this equation reduces to the integral equation version of the nonlinear Poisson-Boltzmann (PB) equation [33]:

$$\nabla^2 \psi = -\frac{1}{\epsilon_0 \epsilon} \sum_{i=1}^2 z_i e \rho_i \exp(-z_i e \psi / k_B T). \quad (7)$$

When R_1 and R_2 are equal in Eq. (1), Eq. (7) is the so-called the Modified Gouy Chapman equation (MGC). On the contrary, if R_1 and R_2 are different in Eq. (1), the nonlinear PB equation corresponds to the unequal-radius MGC (URMGC) equation [24]. Notice that in these quasi point-like ions theories the ionic size is only taken into account partially at the level of a closest approach distance between the macroion and the ions. Contrastingly, in the MC simulations and in the HNC/MSA and HNC/HNC integral equations the ionic size and size asymmetry are incorporated consistently, via the primitive model.

To better understand and characterize the behavior of the SEDL in presence of the electrolytic size asymmetry, from the radial distribution functions, $g_{ij}(r)$, it is possible to calculate two important quantities, namely, the integrated charge (IC)

$$P(r) = z_M + \sum_{i=1}^2 \int_0^r z_i \rho_i g_i(r) 4\pi r^2 dr, \quad (8)$$

and the mean electrostatic potential (MEP)

$$\psi(r) = \frac{e}{4\pi\epsilon_0\epsilon} \int_r^\infty \frac{P(t)}{t^2} dt. \quad (9)$$

When the MEP is evaluated at $r = (D + R_1)/2$ Eq. (9) corresponds to the MEP at the IHP, which we denote as ψ_{IHP} . On the other side, if Eq. (9) is calculated at $r = (D + R_2)/2$ the MEP at the OHP, ψ_{OHP} , is obtained.

With respect to the IC, this quantity is a measure of the total net charge inside a sphere of radius r centered in the macroion. Then, if $D/2 \leq r \leq (D + R_1)/2$ the IC is equal to z_M , whereas for $r \rightarrow \infty$ this quantity goes to zero because of the electroneutrality condition. Furthermore, the IC has also the property of indicating charge reversal when $P(r)z_M < 0$.

C. Numerical simulations

Monte Carlo simulations of the SEDL were performed considering a cubic box with a macroion fixed at the center under periodic boundaries. Due to the electroneutrality condition the following relation was satisfied:

$$N_- z_- + N_+ z_+ + z_M = 0, \quad (10)$$

where N_- and z_- are the number of ions and the valence of the negative species, respectively, N_+ and z_+ are the number of ions and the valence corresponding to the positive species, and z_M is the valence of the macroion, which is related to the surface charge density as $\sigma_0 = z_M e / \pi D^2$.

In order to take into account the long range nature of the coulombic potential, the Ewald sums scheme was adopted, using conducting boundary conditions [40, 41]. The damping constant α was set to $\alpha = 5/L$ and the k -vectors employed to compute the reciprocal space contribution to the energy satisfied the condition $k \leq 5$. The length L of the simulation box was assigned considering a total number of ions $N_t = N_- + N_+ \approx 1000$. After N_t attempts to move an arbitrary ion a Monte Carlo cycle is counted. The thermalization process consisted of 2×10^4 MC cycles, and from 2×10^6 (for high z_M values) to 6×10^6 (for low z_M values) MC cycles were completed in order to calculate the canonical average. The quality of the simulation was tested calculating the IC, which in a region far from the macroion and near of the borders of the simulation box vanished in all cases, as expected.

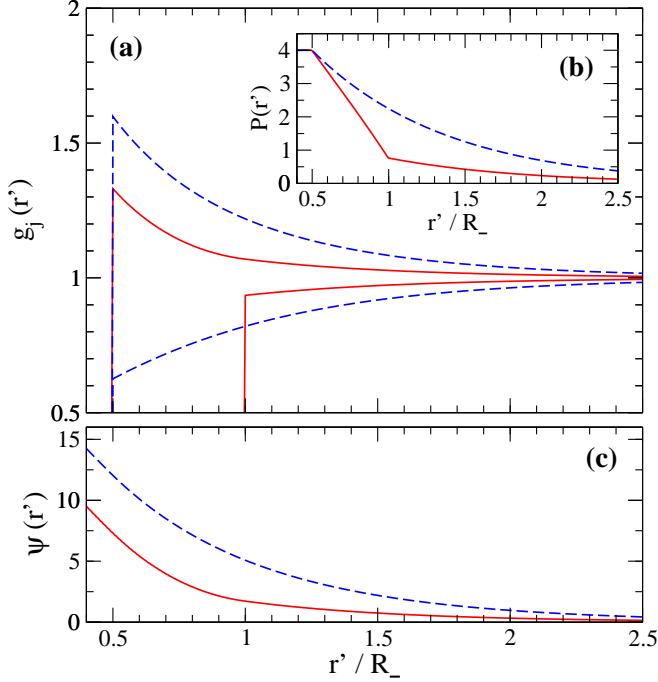


FIG. 1: (Color online:) Radial distribution functions, integrated charge and mean electrostatic potential of a size-symmetric and size-asymmetric 1:1 salt around a charged macroion of valence $z_M = 4$ ($\sigma_0 = 0.05 \text{ C/m}^2$) and diameter $D = 20 \text{ \AA}$ in the PB approach. The solid and dashed lines correspond to URMGC and MGC equations, respectively.

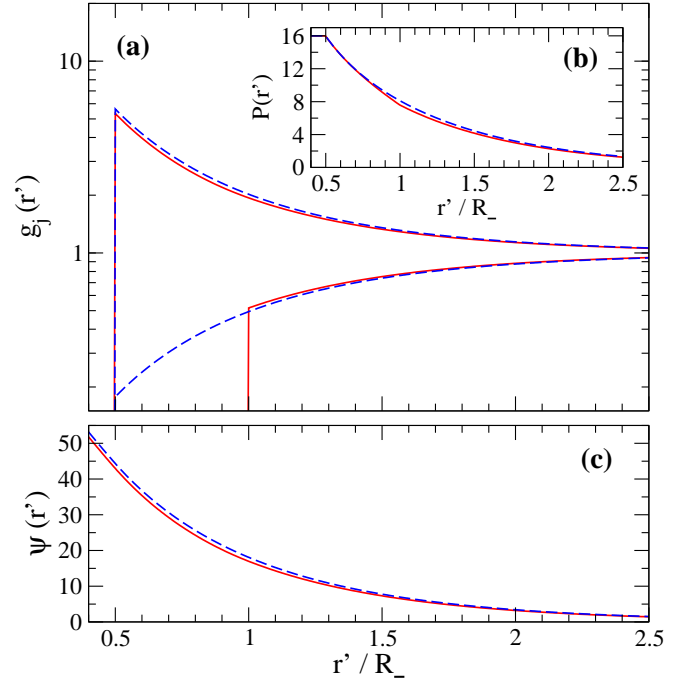


FIG. 2: (Color online:) The same as in Fig. 1 but for $z_M = 16$ ($\sigma_0 = 0.2 \text{ C/m}^2$).

III. RESULTS AND DISCUSSION

A. The role of the ionic size asymmetry in the PB scheme

Physically, in the MGC and URMGC equations the ionic size is considered only partially because the electrolytic ions are allowed to be close to the macroion until a closest approach distance for each species, but the ions interact among them as charged points. Thus, the MGC and URMGC equations correspond, to the simplest manner in which the effects of the ionic size and the size asymmetry can be studied in the EDL, as it was done by Valleau et al. in the 1980s for the planar instance [24]. Notwithstanding, although URMGC represented a step beyond MGC, when the ionic size and in particular the ionic size asymmetry is fully taken into account (as occurs in the MC simulations and in the HNC/MSA and HNC/HNC integral equations) new features absent in PB picture emerge. Therefore, in order to later compare and discuss the consequences of a complete consideration of ionic size asymmetry in the SEDL, we will begin with a review of size asymmetry in the URMGC approach, where the excluded volume effects are embodied partially only in the colloid-ion interactions. Thus, let us first study a spherical macroion of diameter and surface charge density $D = 20 \text{ \AA}$ and $\sigma_0 = z_M e / \pi D^2$, respectively, surrounded by a 1:1, 1 M electrolyte, in a continuum solvent of dielectric constant $\epsilon = 78.5$ at a temperature $T = 298 \text{ K}$. In the size-symmetric case

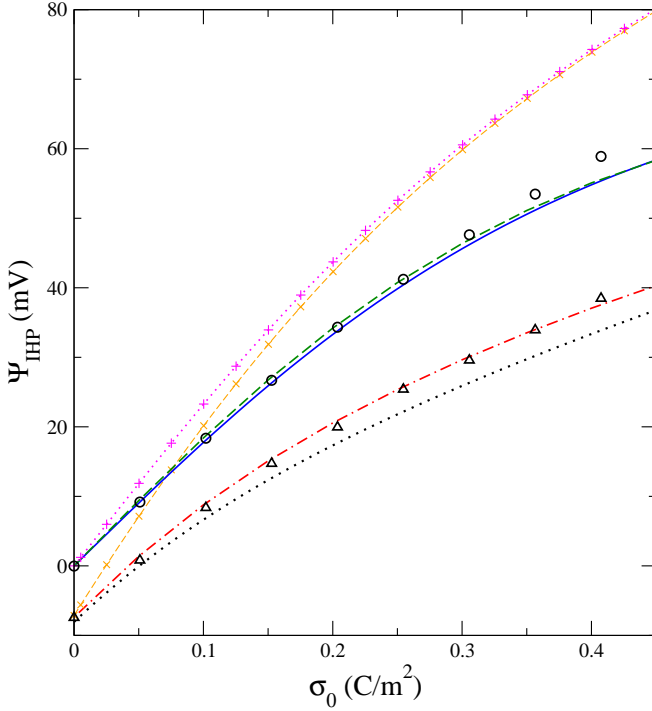


FIG. 3: (Color online:) Mean electrostatic potential at the IHP as function of the surface charge density σ_0 , for a 1:1, 1 M electrolyte around a macroion of diameter $D = 20$ Å. The simulations results were calculated for $z_M = 0, 4, 8, 12, 16, 20, 24, 28$ and 32 . The diameters of the ionic species in the PM are $R_- = 4.25$ Å and $R_+ = 8.5$ Å. In the RPM, the ionic diameters are equal to the counterions in the PM, i.e. 4.25 Å. The maximum approach distances d_{ij} for ion-ion and macroion-ion interactions for theory and simulation are given by Eqs. (11) y (12). The triangles and the circles correspond to Monte Carlo simulation results in the PM, MC_{PM} , and in the RPM, MC_{RPM} , respectively. The dotted and solid lines correspond to HNC/MSA_{PM} and HNC/MSA_{RPM}, and the dot-dashed and dashed lines are associated to HNC/HNC_{PM} and HNC/HNC_{RPM}, respectively. The dashed line with multiplication symbols denotes URMGC and the dotted line with plus symbols is for MGC.

(i.e. for the MGC theory), the maximum approach distance for both species is $4.25/2$ Å, whereas in the size-asymmetric (i.e. for the URMGC theory) is $4.25/2$ Å for anions and $8.5/2$ Å for cations. Since we will consider only $\sigma_0 > 0$ values, in both instances the counterions have the same properties, being the size of the coions the unique difference between the MGC and URMGC systems. Therefore, in Fig. 1 we compare the RDFs, ICs and MEPs curves associated to the size-symmetric and to the size-asymmetric cases, when the valence of the macroion is $z_M = 4$ ($\sigma_0 = 0.05C/m^2$). At the level of the RDFs, in Fig. 1a it is observed that the MGC profiles for the size-symmetric case enclose the RDFs of the size-asymmetric electrolyte described by URMGC. Besides, from Figs. 1b and 1c it is seen that the region not allowed for big cations but accessible for the small anions in the

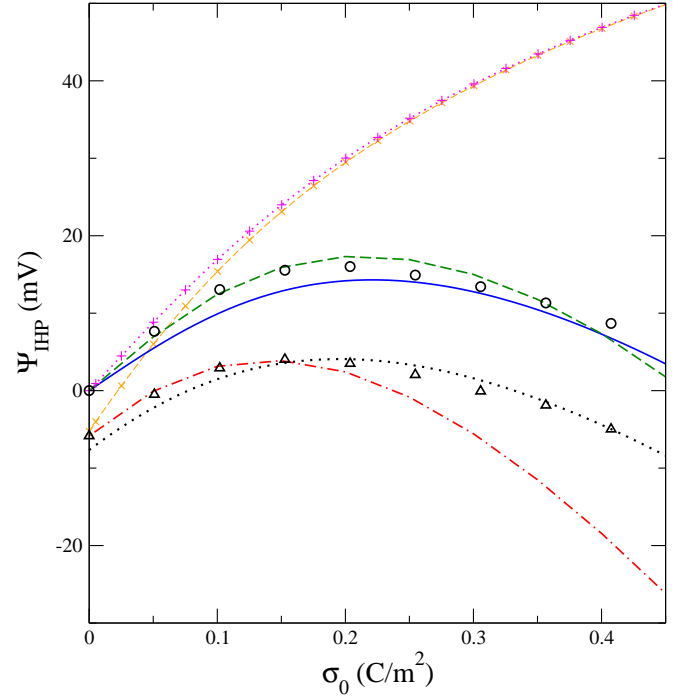


FIG. 4: (Color online:) The same as in Fig. 3 but for a 2:2 electrolyte at 0.5 M concentration.

URMGC theory contributes significantly to the increase of the neutralization and the screening of the spherical EDL when contrasted with the MGC theory (notice that $P(r)_{URMGC} \leq P(r)_{MGC}$ and $\psi(r)_{URMGC} \leq \psi(r)_{MGC}$ for all the r plotted). These differences in the RDFs, $P(r)$, and $\psi(r)$ are expected to augment if z_M decreases, with the largest dissimilarities occurring precisely at the point of zero charge (PZC). Additionally, it is foreseen a MEP equal to zero at the closest approach distance of anions in the MGC results and an electrostatic potential different from zero for URMGC at the same distance. This happens for a $z : z$ salt when $z_M = 0$ because, under these conditions, the RDFs for MGC must coincide for symmetry reasons, while for URMGC the ionic density profiles must be completely different in order to fulfill the electroneutrality condition (i.e. as the macroion is uncharged, only the accumulation of the large ionic species after the OHP can compensate the adsorbed charge of the small ions in between the Helmholtz planes). On the contrary, if z_M increases and there are no crossings between the RDFs of counterions and coions for MGC, and the same behavior is displayed by URMGC, the MGC curves are the limit of URMGC profiles when $z_M \rightarrow \infty$ due again to the electroneutrality condition. Such phenomenon has been already discussed in [33]. Thus, even if, strictly, the MGC and URMGC profiles should not be the same for high z_M values (because there is always a region where the small coions can exist in URMGC, see Fig.2a), the structural properties of the EDL, as the integrated charge and the mean electrostatic potential, are

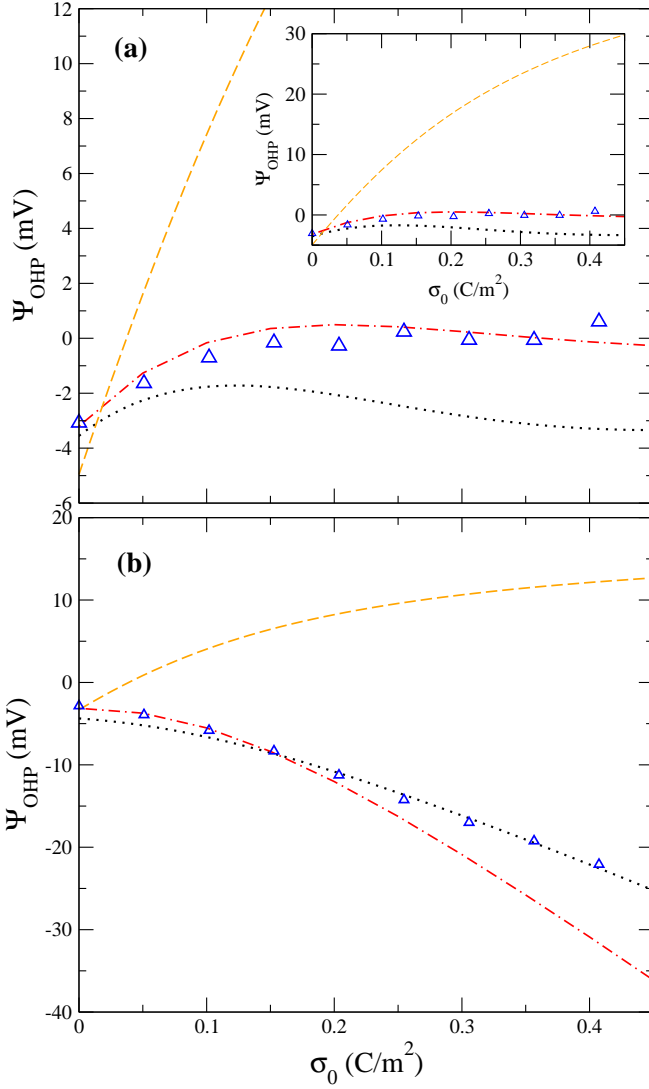


FIG. 5: (Color online:) Mean electrostatic potential at the OHP as function of the surface charge density σ_0 , around a macroion of diameter $D = 20$ Å. The simulation results were calculated for $z_M = 0, 4, 8, 12, 16, 20, 24, 28$ and 32 . The diameters of the ionic species in the PM are $R_- = 4.25$ Å and $R_+ = 8.5$ Å. The maximum approach distances d_{ij} for ion-ion and macroion-ion interactions for theory and simulation are given by Eqs. (11) y (12). The triangles correspond to Monte Carlo simulations. The dotted, dot-dashed and dashed are associated to HNC/MSA_{PM} and HNC/HNC_{PM}, and URMGC, respectively. In Fig. 5a the electrolyte is 1:1, 1 M, whereas in Fig. 5b the salt is 2:2, 0.5 M.

indeed very similar as can be observed in Figs. 2b and 2c. Consequently, far from the PZC the properties of the spherical EDL are expected to be practically the same for URMGC and MGC because the coion's contribution is negligible and the counterions are the same in both cases. This last merging between URMGC and MGC is precisely the so-called dominance of counterions in the spherical EDL and will be of decisive importance in the

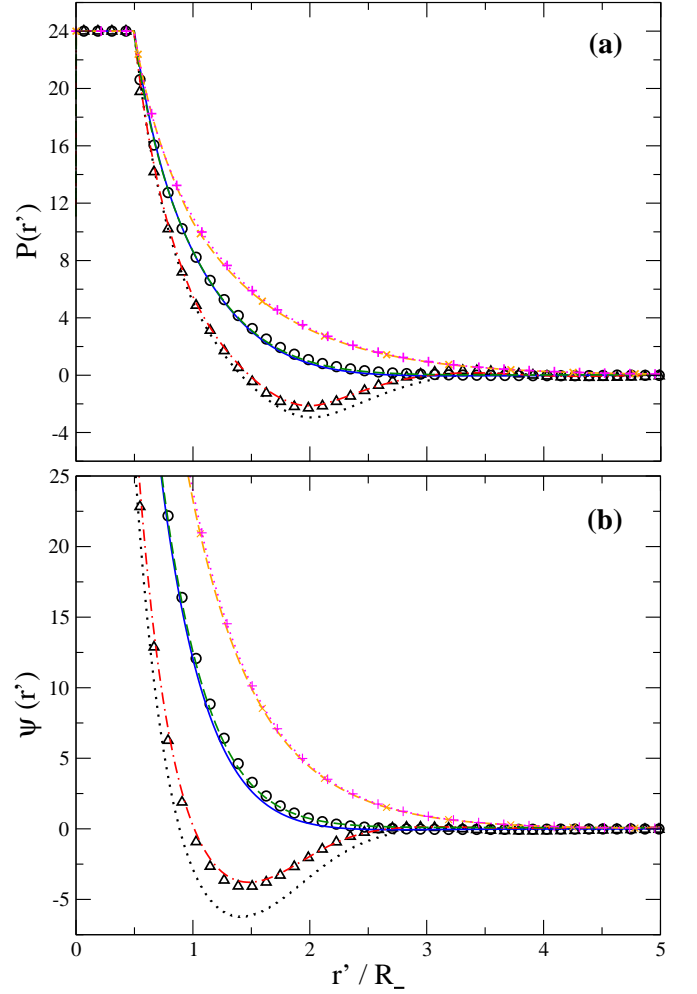


FIG. 6: (Color online:) Integrated charge and mean electrostatic potential as function of the distance for a 1:1, 1 M electrolyte near a macroion of diameter $D = 20$ Å and $z_M = 24$. The diameters of the ionic species in the PM are $R_- = 4.25$ Å and $R_+ = 8.5$ Å. In the RPM, the ionic diameters are equal to the counterions in the PM, i.e. 4.25 Å. The maximum approach distances d_{ij} for ion-ion and macroion-ion interactions for theory and simulation are given by Eqs. (11) y (12). The triangles and the circles correspond to MC_{PM} and MC_{RPM}, respectively. The dotted and solid lines correspond to HNC/MSA_{PM} y HNC/MSA_{RPM}, and the dot-dashed and dashed lines are associated to HNC/HNC_{PM} and HNC/HNC_{RPM}, respectively. The dashed line with multiplication symbols denotes URMGC and the dotted line with plus symbols is for MGC. The distance r' is measured from the macroion's surface.

corresponding potential-charge relationship, as it will be shown later.

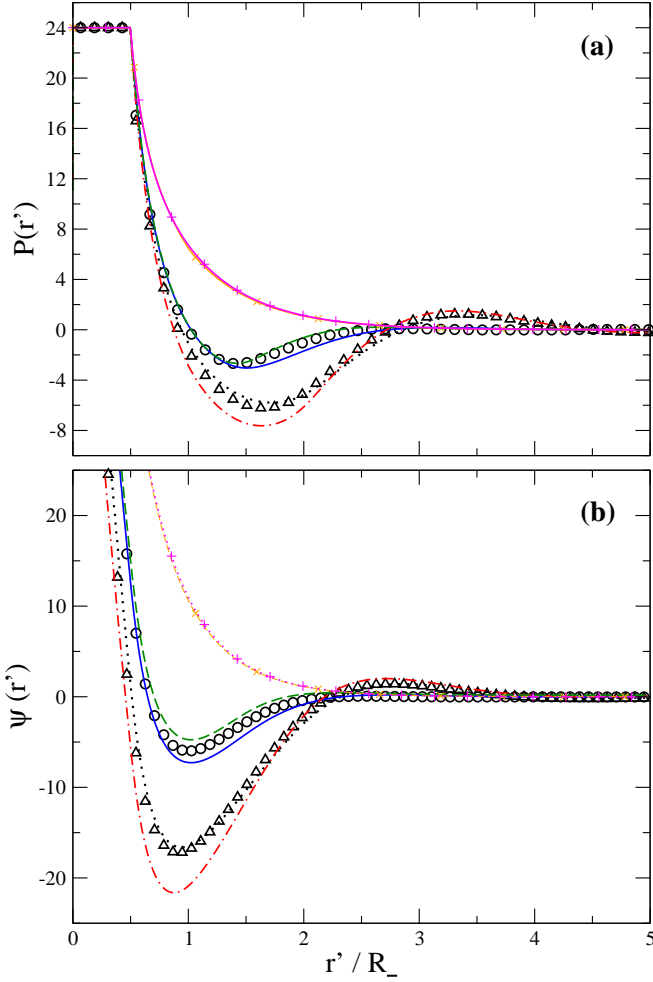


FIG. 7: (Color online:) The same as in Fig. 6 but for a 2:2, 0.5 M salt.

B. The role of the ionic size asymmetry in the primitive model: MC simulations and theoretical results

As discussed, one of the main differences between size-symmetric and size-asymmetric EDLs salt in the PB viewpoint is the increment in the neutralization or screening predicted by URMGC, with respect to MGC, near the PZC. In addition, for high surface charge densities the properties of the SEDL are expected to be practically the same, such as the dominance of counterions arises in a quasi-point like description (i.e. MGC and URMGC).

Now, in this section we will show comprehensive MC data and integral equations (IE) results in which the ionic size asymmetry is taken into account *consistently* in the Eqs. (1) and (2) (and not only at the macroion-ion level as it was done in the nonlinear PB equation of Sec. III A) in order to display the effects in the SEDLs due to a more realistic treatment of size-symmetric and size-asymmetric salts.

In all the following simulations and theoretical calculations we considered a macroion of diameter $D = 20$ Å and $\sigma_0 \geq 0$, immersed in a continuum solvent of dielectric constant $\epsilon = 78.5$ at a temperature $T = 298$ K, in presence of a binary electrolyte. In the primitive model (PM) the *diameter* of the counterions is $R_- = 4.25$ Å and the diameter of coions is the double, i.e. $R_+ = 8.5$ Å. For the restricted primitive model, the size of both species is the same of the counterions in the PM, i.e. 4.25 Å. Thus, the maximum approach distances in the PM and the RPM correspond to those of the electrolyte for URMGC and MGC, respectively. This information is summarized in Eqs. (11) and (12). Notice that the diameter of the macroion and the ionic size asymmetry correspond to values that emphasize the spherical geometry of the EDL and that have been typically used in previous works [30, 33, 42, 43].

Very importantly, the mean electrostatic potential at some distance from the surface of the macroion is frequently associated with the so-called electrokinetic potential at the shear plane (or the zeta potential, ζ) [4]. Such quantity is very relevant in colloidal studies since it is experimentally measurable and allows to characterize and summarize the behavior of the SEDL, as functions of the colloidal charge, in a single potential-charge plot. Furthermore, the zeta potential is used often in physical-chemistry to characterize the macroscopic properties and the stability of charged colloidal dispersions [5, 6]. Given that, in the past, the ψ_{IHP} or the ψ_{OHP} have identified with ζ , we start by showing the $\psi\text{-}\sigma_0$ curves at the IHP and at the OHP for our PM systems. In Fig. 3, MC simulations of the mean electrostatic potential at the IHP for a 1 M, 1:1 electrolyte in the PM and the RPM are shown. The first notable feature there is the *merging* of the MGC and URMGC curves for high σ_0 values. Precisely, this asymptotic conduct illustrates the dominance of counterions at the level of $\psi\text{-}\sigma_0$. Besides, in this figure it is seen that the maximum difference between the MEPs corresponding to MGC and URMGC happens precisely at the PZC, as it had been pointed out in Sec. III A. In strong contrast, the most evident characteristic displayed by the simulational data of ψ_{IHP} for the size-symmetric (RPM) and size-asymmetric (PM) instances is that these curves *do not converge to the same one when σ_0 augments*. This confirms that the counterions do not always dominate the EDL far from the PZC, or, in other words, exemplify the importance of the size of the coions at high colloidal charges, as it was theoretically predicted in Ref. [33]. Additionally, the simulational data shows a potential different from zero at the PZC for the size-asymmetric electrolyte. Clearly, such behavior is due to the fact that the small negative ions are allowed to be closer to the surface than the big positive ions, i.e. for $\sigma_0 = 0$ the negative sign of the MEP at the IHP results from the size asymmetry of the 1:1 electrolyte. Interestingly, analogous results had been theoretically predicted for the RPM planar EDL of charge asymmetric species [38, 44]. However, these data have not been confirmed simulationally. With respect

$$d_i = \begin{cases} d_- = \frac{D+R_-}{2} \text{ and } d_+ = \frac{D+R_+}{2}, & \text{for MC}_{PM}, \text{HNC/MSA}_{PM} \\ & \text{HNC/HNC}_{PM} \text{ and URMGC}; \\ d_- = d_+ = \frac{D+R_-}{2}, & \text{for MC}_{RPM}, \text{HNC/MSA}_{RPM} \\ & \text{HNC/HNC}_{RPM} \text{ and MGC}; \end{cases} \quad (11)$$

$$d_{ij} = \begin{cases} d_{--} = R_- \text{ and } d_{++} = R_+, & \text{for MC}_{PM}, \text{HNC/MSA}_{PM}, \text{HNC/HNC}_{PM}; \\ d_{-+} = d_{+-} = \frac{R_-+R_+}{2}, & \text{for MC}_{PM}, \text{HNC/MSA}_{PM}, \text{HNC/HNC}_{PM}; \\ d_{--} = d_{++} = d_{-+} = d_{+-} = R_-, & \text{for MC}_{RPM}, \text{HNC/MSA}_{RPM} \text{ and HNC/HNC}_{RPM}; \\ d_{--} = d_{++} = d_{-+} = d_{+-} = 0, & \text{for URMGC and MGC}. \end{cases} \quad (12)$$

to the performance of the integral equation theories in the RPM, it is remarkable that both the HNC/HNC and HNC/MSA theories agree with the simulation data, although, for the PM case, HNC/HNC follows closely the MC curves than HNC/MSA.

In addition, in Fig. 3 the MC simulations and integral equations (IE) predict a larger value of σ_0 for which the negative sign of the MEP at the IHP changes to positive than that corresponding to URMGC. This exemplify again the importance of the entropic contributions in the adsorption of counterions between the Helmholtz planes when the ionic size correlations are considered consistently (as occurs in the MC simulations), in contrast with its partial inclusion, when only different approach distances in the macroion-ion interaction are considered, which neglects ionic excluded volume effects outside of the OHP (as in the URMGC theory). Another phenomenon observed in Fig. 3 is that $\psi(\sigma_0)_{PM} < \psi(\sigma_0)_{RPM}$ at the IHP for all σ_0 values plotted. Near the point of zero charge this is explained, in the PM, in terms of the adsorption of negative counterions that are not neutralized by the big coions, as it happens in the RPM case. When σ_0 augments, the positive bare charge overcomes the contribution of the negative counterions near the macroion's surface and the MEP's sign changes from negative to positive as it was mentioned above. Nevertheless, for all the σ_0 values displayed the counterions in the PM provide an extra screening which is not present in the RPM, which leads to the $\psi(\sigma_0)_{PM} < \psi(\sigma_0)_{RPM}$ condition. Moreover, in the monovalent case of the PM this extra screening can be related not only with a higher adsorption of negative counterions with respect to the RPM but also with the presence of charge reversal, that is absent in the RPM. This behavior will be clarified later when the corresponding $P(r)$ profiles be presented.

With the purpose of performing a more stringent test for the theories, in Fig. 4 we present MC simulations of the MEP at the IHP for a 0.5 M, 2:2 electrolyte in the PM and the RPM. In this instance, the features already observed in the simulations of monovalent ions are accentuated. In particular, the most important finding is the corroboration of the non-dominance of counterions for divalent ions. In addition, in the size-asymmetric case a very strong adsorption of negative counterions in

the PM is also observed. The importance of excluded volume effects is evinced by noticing that near the PZC the interval of σ_0 for which the ψ_{IHP} is negative is larger for MC simulations and IE theories than for URMGC. Furthermore, when σ_0 increases after $\psi(\sigma_0)_{PM} > 0$, the ψ_{IHP} reaches a maximum and for still larger σ_0 values $\psi(\sigma_0)_{PM} < 0$ again. The appearance of a maximum in the $\psi(\sigma_0)$ plot for the RPM is related to presence of charge reversal. Besides, the early MEP's change of sign in the PM after the maximum displayed by MC simulations suggests an extra adsorption of counterions with respect to the RPM case, i.e. it is expected an accentuated charge reversal that screens more strongly the positive bare charge of the macroion for high σ_0 values. This behavior will be clearly exhibited in the corresponding $P(r)$ profiles later. On the other hand, the simulational confirmation of the reentrance in the sign of the MEP for divalent ions in the PM, i.e. the double change of sign of ψ_{IHP} , suggests the possibility of observing a corresponding reentrance in the experimental electrophoretic mobility (μ), if the Smolouchowski equation ($\mu = \epsilon\zeta/\eta$) is valid, as it had been theoretically foreseen by HNC/MSA [33] for a larger macroion. This means that the ionic size asymmetry could then cause a reversed mobility in the motion of a macroion in an electrophoresis experiment near the PZC, changing to the "correct" direction when its surface charge density augments, but inverting again its movement at high σ_0 values. Also, notice that for the size-asymmetric instance HNC/HNC shows a better agreement with the simulation data than HNC/MSA for low colloidal charges (when $\sigma_0 \leq 0.16 \text{ C/m}^2$ approximately). Contrastingly, for high surface charge densities ($\sigma_0 > 0.16 \text{ C/m}^2$) the opposite behavior is observed, i.e. a substantial deviation from the MC data is displayed by HNC/HNC, which contrasts with the good accordance shown by HNC/MSA. This conduct is remarkable since, for high colloidal charges and high entropic-electrostatic ionic correlations, in the divalent case HNC/MSA is better than HNC/HNC in opposition to the univalent instance.

In Fig. 5 the simulational results of the MEP at the OHP, ψ_{OHP} , for the PM monovalent and divalent salts are plotted. As we said before, the importance of the study of this curves arises from the fact that the ψ_{OHP} could be identified with the zeta potential (ζ). In Fig.

5a, which corresponds to the 1:1, 1 M electrolyte, a non-monotonic behavior of the MEP as a function of σ_0 is observed. This conduct is reproduced correctly by IE theories, with HNC/HNC showing a better agreement than HNC/MSA. Contrastingly, URMGC presents a monotonic behavior, which completely differs from the simulation data, and predicts large values of the electrostatic potential for high σ_0 as it can be seen in the inset. The simulational results of ψ_{OHP} for the 2:2, 0.5 M electrolyte are portrayed in Fig. 5b. Here, in the MC simulations it is observed that for any value of σ_0 the ψ_{OHP} is negative and decreases monotonically as a function of σ_0 . A similar curvature has been theoretically predicted in the RPM spherical EDL by one of the present authors for a macroion of diameter $D = 80 \text{ \AA}$ immersed in a 2:2, 0.5 M electrolyte of ionic diameter equal to 7 \AA [21], at approximately the same volume fraction used here in our PM. Thus, the simulational results presented in this work corroborate that such anomalous curvatures in the MEP, at high ionic volume fractions, are a real feature in the primitive model. Even if this phenomenon is interesting just from the theoretical point of view [45, 46, 47], could also be relevant in the description of non-intuitive attributes of double layer systems such as the occurrence of negative differential capacitances [47, 48, 49, 50, 51, 52]. Once again, the whole behavior displayed by the simulations is well captured by the IE theories, although now HNC/MSA is closer to simulations than HNC/HNC. Contrastingly, URMGC exhibits a monotonic behavior in which the MEP increases as a function of σ_0 , as occurred in the 1:1 instance.

As was noticed for the $\psi(\sigma_0)$ relationship, one of the consequences of the ionic size asymmetry in the PM electrical double layer, is the enhancement of the neutralization and screening at high surface charges. To illustrate this in terms of the ionic charge adsorption, in Fig. 6a we have plotted the integrated charge profiles for the 1:1, 1 M electrolyte in the PM and RPM, when the macroion's valence is $z_M = 24$. Here, it is clearly seen that the ionic size asymmetry not only promotes a higher adsorption of counterions, i.e. $P(r)_{PM} \leq P(r)_{RPM}$, but also that can *induce the appearance of charge reversal in monovalent electrolytes*, showing a minimum at $r'/R_- \approx 2$. Consequently, MC simulations hint that charge reversal can occur even in presence of monovalent salts whenever the high coupling conditions are present, i.e. high electrolyte concentration or large hydration of the electrolyte. Note that the IE theories reproduce very well the charge reversal behavior, whereas an incorrect monotonic decrease of the IC is shown by URMGC.

The overcompensation of the native charge in the PM is also reflected in the corresponding MEP curves as a function of the distance as can be verified in Fig. 6b. In this case the monotonicity of the $\psi(r)_{RPM}$ and the non-monotonic behavior of $\psi(r)_{PM}$ can be easily deduced from the corresponding $P(r)$ profiles and the Eq. (9). In particular, note that the condition $P(r)_{PM} \leq P(r)_{RPM}$ implies that $\psi(r)_{PM} \leq \psi(r)_{RPM}$ for MC simulations and

HNC/HNC and HNC/MSA theories, i.e. to a higher neutralization of the macroion's bare charge (as observed in $P(r)$) a higher screening in $\psi(r)$ is associated.

In the Fig. 7a the charge adsorption for a 2:2, 0.5 M electrolyte as function of the distance in the PM and RPM is displayed when the valence of the macroion is $z_M = 24$. Notice that the integrated charge simulation curve shows that in the RPM electrical double layer there is charge reversal, contrasting with the behavior of the 1 M monovalent case previously portrayed, where it was found the absence of this feature even for a higher electrolytic concentration. Besides, when the ionic size asymmetry is present in the PM the charge reversal, already observed in the RPM, is notably enhanced. This illustrates the fact that *the high electrostatic-entropic coupling conditions for which the charge reversal appears can be relaxed for multivalent salts*, i.e., it is expected that for $1 : z$ salts the ionic size and/or the ionic size asymmetry (coming from the ionic hydration for example) become very important even at moderate salt concentrations reachable experimentally, as it has been reported by several experimental works [53, 54, 55, 56, 57]. The MEP curves corresponding to the IC profiles discussed previously now are plotted in Fig. 7b. Consistently, the MC simulations and the HNC/HNC HNC/MSA theories predict that near the macroion's surface the screening in the PM is higher than in the RPM, with the MEP presenting a non-monotonic behavior in both cases. Furthermore, here it is noticed that the overestimation of the screening in the HNC/HNC potential profile has its origin in the charge overcompensation displayed by the corresponding $P(r)$ graphed in Fig. 7a.

IV. CONCLUDING REMARKS

Monte Carlo simulations of the primitive model spherical electrical double layer, in the presence of either monovalent or divalent salts, were performed and compared with data of the HNC/HNC and HNC/MSA integral equations and of the MGC and URMGC quasi-punctual-ions schemes. One of the most simple manners in which the ionic size and size asymmetry can be taken into account *partially* in the EDL is via the MGC and URMGC approaches, in which the excluded volume effects are considered solely in the macroion-ion interactions by means of a closest approach distance. When size-symmetric and size-asymmetric semi-punctual EDLs (i.e. systems with either equal or different closest approach distances for the otherwise-punctual electrolytic species) with the same type of counterions are considered by the MGC and URMGC formalisms, respectively, it was exhibited here that, at low colloidal charges, one of the main effects of including the ionic size asymmetry in the URMGC theory is an enhancement of the screening and the neutralization in the EDL with respect to the MGC (or size-symmetric) instance. On the other hand, far from the point of zero charge, it was shown that the

RDFs, ICs, and MEPs predicted by the MGC and URMGC equations displayed always a monotonic comportment, and that the ionic distributions almost coincided for all the values of r , with exception, maybe, of the zone comprised between the Helmholtz planes. However, as $\sigma \rightarrow \infty$, the differences between the MGC and URMGC radial distribution functions, and therefore between all their concomitant structural and thermodynamic properties, go asymptotically to zero. This behavior is the so-called dominance of the counterions. Contrastingly, when the ionic finite size and size asymmetry are embodied consistently into the macroparticle-ion and ion-ion interactions, as occurred in the Monte Carlo (MC) simulations and the HNC/HNC and HNC/MSA integral equations, several characteristics absent in the nonlinear Poisson-Boltzmann data (e.g. the non-monotonic behavior of the RDFs, ICs, and MEPs and the phenomenon of charge reversal) emerge. Most importantly, our MC simulations of the primitive model EDL corroborated the fact that the ionic size asymmetry augments the colloidal charge neutralization and the screening in comparison with the size-symmetric case even at high values of σ_0 , *proving the non-dominance of the counterions in the primitive model*. On the theoretical side, the HNC/HNC and HNC/MSA integral equations displayed consistent results with MC simulations, without a notable predominance in the accuracy between them, whereas MGC and URMGC evidenced the limitations of the Poisson-Boltzmann theories. Other consequences of the ionic size asymmetry in the EDL that have been confirmed by the present numerical simulations and HNC/HNC and HNC/MSA calculations are the appearance of charge reversal in monovalent salts and the reentrance of the mean electrostatic potential at the outer Helmholtz plane (i.e., the change of sign of the ψ_{OHP} from negative to positive and, then, to negative again when σ_0 increases from zero) for divalent salts. If the usual identification between the well-known electrokinetic zeta potential and the mean electrostatic potential

in the neighborhood of the Helmholtz region is assumed [2], such reentrance in ψ_{OHP} could be of relevance for mobility experiments since it indicates the possibility of observing an alternating direction in the electrophoresis of a colloid, immersed in a multivalent electrolytic bath, as a function of the native macroparticle's charge. Furthermore, the reported MC simulations have also evinced that anomalous curvatures can appear at the OHP in the primitive model EDL, which could be important for several recent investigations about non-intuitive phenomena (e.g., the appearance of negative differential capacitances [47, 48, 49, 50, 51, 52]) in electrolyte-electrode systems. In summary, the data reported in this paper suggest that the ionic size and, especially, the ionic size asymmetry should be considered as very sensitive parameters that, in combination with the concentration and valence of the electrolyte and the macroion's surface charge density, control the electrostatic-entropic coupling in the primitive model EDL. In particular, given that for multivalent salts the ionic hydration augments notably the finite size and size asymmetry effects, this could represent a way to attain a high electrostatic-entropic coupling at reasonable experimental conditions for which the charge reversal could be detected [53, 54, 55, 56, 57].

Acknowledgments

This work was supported by Consejo Nacional de Ciencia y Tecnología (CONACYT, México), through grants CB-2006-01/58470 and C01-47611, and PROMEP. E. G.-T. thanks to Centro Nacional de Supercómputo of Instituto Potosino de Investigación Científica y Tecnológica for the computing time in the Cray XD1 and IBM E-1350 machines. G. I. G.-G. acknowledges postdoctoral fellowship from CONACYT.

-
- [1] S. S. Dukhin and B. V. Derjaguin, *Surface and Colloid Science* (E. Matijevic, Ed.), Vol. 7, Chaps. 1 and 2 (Wiley, New York, 1974).
 - [2] R. J. Hunter, *Zeta Potential in Colloid Science* (Academic Press, New York, 1981).
 - [3] R. D. Vold and M. J. Vold, *Colloid and Interface Chemistry* (Addison-Wesley, Reading, MA, 1983).
 - [4] R. J. Hunter, *Foundations of Colloid Science* (Clarendon, Oxford, 1987).
 - [5] F. Fenell-Evans and H. Wennerström, *The Colloidal Domain: Where Physics, Chemistry, Biology and Technology Meet* (Wiley-VCH, New York, 1994).
 - [6] P. C. Hiemenz and R. Rajagopalan, *Principles of Colloid and Surface Chemistry* (Marcel Dekker, New York, 1997).
 - [7] S. L. Carnie, D. Y. C. Chan, D. J. Mitchell, and B. W. Ninham, *J. Chem. Phys.* **74**, 1472 (1981).
 - [8] C. N. Patra and S. K. Ghosh, *Phys. Rev. E* **47**, 4088 (1993).
 - [9] C. N. Patra, *J. Chem. Phys.* **111**, 9832 (1999).
 - [10] C. N. Patra and S. K. Ghosh, *J. Chem. Phys.* **117**, 8938 (2002).
 - [11] L. B. Bhuiyan, C. W. Outhwaite, and D. Henderson, *J. Chem. Phys.* **123**, 034704 (2005).
 - [12] F. Jiménez-Ángeles and M. Lozada-Cassou, *J. Chem. Phys.* **128**, 174701 (2008).
 - [13] E. Gonzales-Tovar, M. Lozada-Cassou, and D. Henderson, *J. Chem. Phys.* **83**, 361 (1985); *ibid.* **87**, 5581 (1987).
 - [14] F. Jiménez-Ángeles, G. Odriozola, and M. Lozada-Cassou, *J. Chem. Phys.* **124**, 134902 (2006).
 - [15] T. Goel, C. N. Patra, S. K. Ghosh, and T. Mukherjee, *J. Chem. Phys.* **129**, 154707 (2008).
 - [16] T. Goel, C. N. Patra, S. K. Ghosh, and T. Mukherjee, *J. Chem. Phys.* **129**, 154906 (2008).
 - [17] E. González-Tovar and M. Lozada-Cassou, *J. Phys. Chem.* **93**, 3761 (1989).

- [18] C. W. Outhwaite and L. B. Bhuiyan, *Mol. Phys.* **74**, 367 (1991).
- [19] R. Messina, E. González-Tovar, M. Lozada-Cassou, and C. Holm, *Europhys. Lett.* **60**, 383 (2002).
- [20] F. Jiménez-Ángeles, R. Messina, C. Holm, and M. Lozada-Cassou, **119**, 4842 (2003).
- [21] E. González-Tovar, F. Jiménez-Ángeles, R. Messina, and M. Lozada-Cassou, *J. Chem. Phys.* **120**, 9782 (2004).
- [22] Y. X. Yu, J. Z. Wu, and G. H. Gao, *J. Chem. Phys.* **120**, 7223 (2004).
- [23] T. Goel and C. N. Patra, *J. Chem. Phys.* **127**, 034502 (2007).
- [24] J. P. Valleau and G. M. Torrie, *J. Chem. Phys.* **76**, 4623 (1982).
- [25] L. B. Bhuiyan, L. Blum, and D. Henderson, *J. Chem. Phys.* **78**, 442 (1983).
- [26] J. J. Spitzer, *J. Colloid Interface Sci.* **92**, 198 (1983).
- [27] A. F. Khater, D. Henderson, L. Blum, and L. B. Bhuiyan, *J. Phys. Chem.* **88**, 3682 (1984).
- [28] U. Marini Bettolo Marconi, J. Wiechen, and F. Forstmann, *Chem. Phys. Lett.* **107**, 609 (1984).
- [29] C. W. Outhwaite and L. B. Bhuiyan, *J. Chem. Phys.* **84**, 3461 (1986).
- [30] H. Greberg and R. Kjellander, *J. Chem. Phys.* **108**, 2940 (1998).
- [31] M. Valiskó, D. Henderson, and D. Boda, *J. Phys. Chem. B* **108**, 16548 (2004).
- [32] D. Gillespie, M. Valiskó, and D. Boda, *J. Phys.: Condens. Matter* **17**, 6609 (2005).
- [33] G. I. Guerrero-García, E. González-Tovar, M. Lozada-Cassou, and F. de J. Guevara-Rodríguez, *J. Chem. Phys.* **123**, 034703 (2005).
- [34] K. Wang, Y.-X. Yu, G.-H. Gao, and G.-S. Luo, *J. Chem. Phys.* **123**, 234904 (2005).
- [35] M. Valiskó, D. Boda, and D. Gillespie, *J. Phys. Chem. C* **111**, 15575 (2007).
- [36] K. Wang, Y.-X. Yu, G.-H. Gao, and G.-S. Luo, *J. Chem. Phys.* **126**, 135102 (2007).
- [37] S. L. Carnie and G. M. Torrie, *Adv. Chem. Phys.* **56**, 141 (1984).
- [38] L. B. Bhuiyan and C. W. Outhwaite, *Phys. Chem. Chem. Phys.* **6**, 3467 (2004).
- [39] G. N. Patey, *J. Chem. Phys.* **72**, 5763 (1980).
- [40] M. P. Allen and D. J. Tildesley *Computer Simulation of Liquids* (Oxford University Press, New York, 1989).
- [41] D. Frenkel and B. Smit *Understanding Molecular Simulation* (Academic Press, London, 2002).
- [42] J. Z. Wu, D. Bratko, H. W. Blanch, and J. M. Prausnitz, *J. Chem. Phys.* **111**, 7084 (1999).
- [43] T. Terao and T. Nakayama, *Phys. Rev. E* **63**, 041401 (2001).
- [44] D. Boda, D. Henderson, P. Plaschko, and R. Fawcett, *Mol. Simul.* **30**, 137 (2004).
- [45] L. Blum, J. L. Lebowitz, and D. Henderson, *J. Chem. Phys.* **72**, 4249 (1980).
- [46] L. Blum and D. Henderson, *J. Chem. Phys.* **74**, 1902 (1981).
- [47] P. Attard, D. Wei, and G. N. Patey, *J. Chem. Phys.* **96**, 3767 (1992).
- [48] G. M. Torrie, *J. Chem. Phys.* **96**, 3772 (1992).
- [49] M. B. Partenskii and P. C. Jordan, *J. Chem. Phys.* **99**, 2992 (1993).
- [50] M. B. Partenskii and P. C. Jordan, *Condens. Matter Phys.* **8**, 397 (2005).
- [51] M. S. Kilic and M. Z. Bazant, *Phys. Rev. E* **75**, 021502 (2007).
- [52] M. B. Partenskii and P. C. Jordan, *Phys. Rev. E* **77**, 061117 (2008).
- [53] A. Martín-Molina, M. Quezada-Pérez, F. Galisteo-González, and R. Hidalgo-Álvarez, *J. Phys. Chem. B* **106**, 6881 (2002).
- [54] K. Besteman, M. A. G. Zevenbergen, H. A. Heering, and S. G. Lemay, *Phys. Rev. Lett.* **93**, 170802 (2004).
- [55] K. Besteman, M. A. G. Zevenbergen, and S. G. Lemay, *Phys. Rev. E* **72**, 061501 (2005).
- [56] A. Fernández-Nieves, A. Fernández-Barbero, and F. J. de las Nieves, *J. Chem. Phys.* **123**, 054905 (2005).
- [57] F. H. J. van der Heyden, D. Stein, K. Besteman, S. G. Lemay, and C. Dekker, *Phys. Rev. Lett.* **96**, 224502 (2006).